Polymer 50 (2009) 945–952

Contents lists available at ScienceDirect

Polymer

journal homepage: www.elsevier.com/locate/polymer

Multi-scale modeling of cross-linked epoxy nanocomposites

Suyoung Yu, Seunghwa Yang, Maenghyo Cho*

School of Mechanical and Aerospace Engineering, Seoul National University, San 56-1, Shillim-Dong, Kwanak-Ku, Seoul 151-744, Republic of Korea

ARTICLE INFO

Article history:
Received 3 September 2008
Received in revised form
21 November 2008
Accepted 21 November 2008
Available online 10 December 2008

Keywords:
Nanocomposites
Micromechanics
Molecular dynamics

ABSTRACT

The effect of different sized alumina (Al_2O_3) nanoparticles on the mechanical properties of thermoset epoxy-based nanocomposites is investigated using molecular dynamic (MD) simulations combined with sequential scale bridging methods. In molecular structures, the cross-linked networking effect of the pure EPON862®–TETA® polymer has been independently considered and validated by MD simulations. Based on the validation of pure epoxy structures, nanocomposites' unit cells, consisting of spherical Al_2O_3 particles and epoxy, have been constructed. In order to investigate the particle size effects, various unit cells having different particle radii but the same volume fraction have been considered and simulated. The mechanical properties of the nanocomposites are calculated using the Parrinello–Rahman fluctuation method to give an enhanced reinforcing effect in smaller particle reinforced cases. Based on the MD simulation results, the sequential bridging method is adopted for efficient estimation of the particle size and epoxy networking effects. An effective interface concept is incorporated as a characteristic phase which can describe the particle size effects. The values calculated from the micromechanics model are in good agreement with those of the molecular dynamics simulations.

1. Introduction

Recently, various types of nanoparticulate composites have been developed and studied for their potential applications [1–4]. When the size of fillers in composites decreases to a nanometer scale, the ratio of their surface area to volume increases critically and this enables unusual mechanical properties, which are different from those of their macro-sized counter parts [5]. Due to the large variation in the surface to volume ratios at the nanometer scale, the material properties of nanocomposites are very sensitive to the size of the nanoparticles. Therefore, the demands for the establishment of efficient analysis tools, with rigorous considerations of atomistic structures and their effects on the macro properties, have become crucial and challengeable tasks in the design of nanocomposites.

Polymeric structures are divided into two types, namely thermoplastic and thermoset polymers. The application of both types of polymers as matrix materials can result in different properties, including the size effects of nanocomposites, because thermoset polymers have a distinct structure called 'cross-linked networks' between the polymer chains. Due to the strong covalent bonding between individual chains, thermoset epoxy resins exhibit excellent properties used as the matrix of many composites materials.

Recently, several theoretical studies, based on the understanding of the atomistic behaviour of polymeric structures, have contributed to the modeling and characterization of thermoset polymers [6–10]. Wu and Xu [6,7] developed a method for the construction of a polymer network between diglycidyl ether bisphenol A (DGEBA) and isophorone diamine (IPD). The polymer network, with conversion up to 93.7%, was successfully generated and elastic constants and density were estimated from the equilibrated structure via MD simulations. Hamerton et al. [8] proposed the effects of a cross-linked structure on the thermo-mechanical properties of epoxy, by MD simulations. Yarovsky and Evans [9] developed three different models to reduce the molecular weight of water soluble cross-linked epoxy resins. And Komarov et al. [10] developed a coarse-grained model using a mapping/reverse-mapping procedure for the cross-linked polymers. In their approaches, due to the reduction of the degrees of freedoms to be solved in the MD simulations, a unit cell of large problem can be composed and thermal properties such as density, glass transition temperature (T_g) and the thermal expansion coefficient of large cross-linked epoxy structures can be obtained.

On the other hand, in the case of using molecular models of polymer nanocomposites with epoxy matrices [11,12], both the epoxy resin and the curing agent can be independently modeled and no direct cross-linking is normally considered. Also, the details of the formation of the cross-linked network between the epoxy

* Corresponding author. Tel.: +82 02 880 1693; fax: +82 02 886 1645.
E-mail address: mhcho@snu.ac.kr (M. Cho).

0032-3861/$ – see front matter © 2008 Elsevier Ltd. All rights reserved.
doi:10.1016/j.polymer.2008.11.054

resin and the curing agent are neglected, and the linkage of the final cured structure is arbitrarily assembled [13]. Considering the fact that the formation of an adsorption layer surrounding the reinforcing fiber can be critically affected by the cross-linked network of the matrix polymers, the exclusion of a cross-linked structure cannot accurately describe the actual cured nanostructures formed by the nanocomposites and the particle size effects at the interface between the particle and the matrix. Therefore cross-linked structures of the thermoset matrix in nanocomposites need to be rigorously considered in MD simulations.

For designing nanocomposites, an efficient analytical method should also be undertaken in order to correlate the overall reinforcing effect and atomistic structures of composites materials such as cross-linked networks. As was used in previous studies, MD simulations which can accurately describe the chemical structure as well as estimate the mechanical properties is useful analytical method for nanomaterials such as nanocomposites. However, MD simulations can be computationally expensive and not worth performing when designing materials or characterizing large scale simulations such as nanocomposites with particle sizes larger than 10 nm. So various approaches for multi-scale analysis such as micromechanics method have been developed [4,14], but a conventional micromechanical method such as the Mori–Tanaka model [15] does not accurately describe the particle size effects. Therefore, an efficient scale bridging method considering the size of the nanocomposites needs to be applied.

In this study, the effect of the nanoparticles' size on the mechanical properties of thermoset polymer matrix-based nanocomposites is investigated by MD simulations and a sequential scale bridging method. The paper is organised as follows: in Section 2, an MD simulation methodology, including the forcefield and ensemble simulations, to obtain mechanical properties, is explained. In Section 3, the cross-linked epoxy structure is described and its properties are estimated using MD simulations. In this study, Diglycidyl Ether of Bisphenol F (EPON862®) is chosen as an epoxy unit monomer and Triethylenetetramine (TETA®) is chosen as the curing agent. In Section 4, based on the cross-linked structures obtained in Section 3, molecular modeling of alumina (Al_2O_3)/cross-linked epoxy nanocomposites is introduced, and the relation between the particle size and the reinforcing effects is studied via MD simulations. In Section 5, the micromechanics model, including the effects of the molecular size on the epoxy/alumina nanocomposites, is adopted and compared with MD simulated results.

2. Molecular dynamics methodology

2.1. Forcefield

In order to construct the initial molecular structures and implement all ensemble simulations and post-processes, the commercial molecular simulation program Material Studio® 4.2 [16] has been used, and *ab initio* Condensed-phase Optimized Molecular Potentials for Atomistic Simulation Studies (COMPASS) forcefield was applied to describe inter- and intra-atomic interactions, as the following.

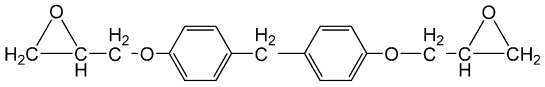

Fig. 1. EPON862® including two epoxide groups of triangular shape. The epoxide groups are the curing sites.

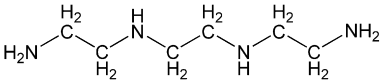

Fig. 2. TETA® consists of 4 nitrogens and six carbons. The nitrogen groups (NH, NH_2) are the curing sites.

$$
\begin{aligned}
E_{\text{total}} = & \sum_b \left[k_2(b-b_o)^2 + k_3(b-b_o)^3 + k_4(b-b_o)^4\right] \\
& + \sum_\theta \left[k_2(\theta-\theta_o)^2 + k_3(\theta-\theta_o)^3 + k_4(\theta-\theta_o)^4\right] \\
& + \sum_\phi [k_1(1-\cos\phi) + k_2(1-\cos 2\phi) + k_3(1-\cos 3\phi)] \\
& + \sum_\chi k_2\chi^2 + \sum_{b,b'} k(b-b_o)(b'-b'_o) \\
& + \sum_{b,\theta} k(b-b_o)(\theta-\theta'_o) + \sum_{b,\phi} k(b-b_o)[k_1\cos\phi \\
& + k_2\cos 2\phi + k_3\cos 3\phi] + \sum_{\theta,\phi} (\theta-\theta_o)[k_1\cos\phi \\
& + k_2\cos 2\phi + k_3\cos 3\phi] + \sum_{b,\theta} k(\theta'-\theta'_o)(\theta-\theta_o) \\
& + \sum_{\theta,\theta',\phi} k(\theta'-\theta'_o)(\theta-\theta_o)\cos\phi + \sum_{i,j}\frac{q_i q_j}{r_{ij}} \\
& + \sum_{i,j}\varepsilon_{ij}\left[2\left(\frac{r^o_{ij}}{r_{ij}}\right)^9 - 3\left(\frac{r^o_{ij}}{r_{ij}}\right)^6\right]
\end{aligned}
\tag{1}
$$

Here, the first four terms are bond stretching, bending, torsion, and out-of-plane potentials, known as the valence term. The next six terms are the cross terms describing the interactions between each valence term, and the last two terms are the non-bonded coulomb and van der Waals potentials. In calculating the non-bonded potentials, the atom-based summation with a cutoff radius of 9.5 Å was used in the van der Waals summation with long range correction. Electrostatic interaction by Coulomb potential can be calculated using the Ewald summation method, but the method requires excessive computing cost. As an alternative for the Coulomb potential, the distance-dependent dielectric constant method with the dielectric value of 2.5 r_{ij} was adopted [17].

2.2. Production run for elastic constants

In the MD simulations, the mechanical properties of all atomistic unit cells are calculated using the Parrinello–Rahman fluctuation method [18,19] where uniform external stress is applied to the unit cell and the deviations of the resultant strain values at each simulation step are monitored. In this simulation, external stress equivalent to the atmospheric pressure (1 atm) is applied to the normal directions in all planes of the unit cell. All the components of the stiffness matrix can be obtained from the fluctuation formulation given below. During the *NσT* (constant stress) ensemble, the ensemble average of the strain perturbations is determined from the

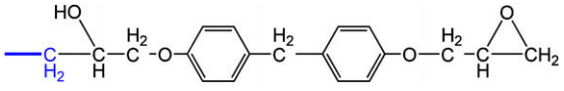

Fig. 3. EPON862® molecule in an active atom (carbon in blue). Carbon atom separated from the oxygen having one free radical can react with nitrogen atom of TETA® molecule under active condition. (For interpretation of the references to colour in this figure legend, the reader is referred to the web version of this article.)

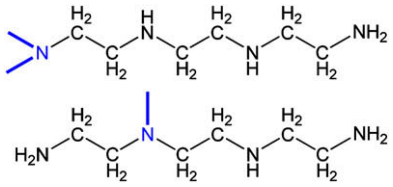

Fig. 4. TETA® under active atom (nitrogen in blue). Nitrogen atom with one free radical can be linked to the active oxygen in EPON862®, 6 in total. (For interpretation of the references to colour in this figure legend, the reader is referred to the web version of this article.)

deformation tensor and the metric tensor, and the stiffness matrix of the unit cell can be calculated as shown below

$$\sigma_{ij} = C_{ijkl}\varepsilon_{kl} \tag{2}$$

$$C_{ijkl} = \frac{kT}{\langle V\rangle}\langle \delta\varepsilon_{ij}\delta\varepsilon_{kl}\rangle^{-1} \tag{3}$$

where k is Boltzman's constant, T is the temperature during the ensemble and $\langle V\rangle$ is the ensemble average of the cell volume.

3. Molecular dynamics simulation of cross-linked epoxy

3.1. Atomistic structures of resin and curing agent

Prior to the modeling of the nanocomposites unit cells, the atomistic structures of pure epoxy and its cross-linking mechanism were first considered. The epoxy resin is composed of EPON862® as the epoxy and TETA® as the curing agent, and the chemical structures of each molecule are shown in Figs. 1 and 2 respectively. The cross-linked networks are built up between the curing sites of epoxy and curing agents. The curing site of epoxy is the epoxide group and the nitrogen groups (NH, NH_2) are the curing sites of the curing agents. There are 2 and 6 curing sites in single EPON862® and TETA® molecules respectively.

3.2. Cross-linking simulation

Cross-links are covalent bond linkages between one polymer chain and another, and the curing reaction is an irreversible chemical reaction. The cross-linking reaction of the EPON862® and TETA® can occur between the active atoms of each molecules, the carbon of the EPON862®, and the nitrogen groups of the TETA® as shown in Figs. 3 and 4.

Table 1
Comparison between simulation values and experimental values.

	Simulation values			Experimental values [21]
	Cross-link producing method	Representative molecule method	Previous study [20]	
Young's modulus [GPa]	3.548	3.362	3.43	3.24
Shear modulus [GPa]	1.296	1.222	–	–
T_g [K]	–	388	378	378

In order to describe the curing reaction between the epoxy resin and curing agent, a unit cell consisting of 12 molecules of EPON862® and 4 molecules of TETA® was constructed. The composition of EPON862® and TETA® is based on the weight ratio (100:15.4). Initial molecules in the cell have no cross-linked bonds. At first, NVT (isothermal) ensemble simulations at high temperature, 500 K, were implemented to give sufficient kinetic energy to all atoms in the cell. During the NVT ensemble simulation studies, atoms of curing pairs move closer to each other as a result of intramolecular interactions described by the COMPASS forcefield. Then, pairs of atoms, whose distance is shorter than the reaction cutoff distance, were selected and connected (i.e. new covalent bonding is created and the forcefield parameters of the newly bonded atoms are automatically changed). The reaction cutoff distance commonly ranges from 4 Å to 10 Å [6]; for this study it was set to 5 Å. Throughout the sequence of these steps, 12 new cross-linked bonds were created and the cross-link ratio of 0.5 was obtained. Besides these methods for cross-linked molecular structures, Monte Carlo simulation can be considered for more exact and actual molecular structures of cross-linked network but it was not considered in the present study.

3.3. Representative cross-linked unit

The cross-link producing method used in Section 3.2 is too complex to be applied to larger models. Therefore, one cross-linked epoxy unit obtained from the previous cross-linking simulation was chosen as a representative molecule for performing more efficient simulation studies. The single cross-linked epoxy unit is composed of three molecules of EPON862® and one molecule of TETA® with the same composition ratio as shown in Fig. 5. The unit has three cross-linked bonds with the cross-linking ratio of 0.5. In order to validate the present representative molecule method, Young's modulus and glass transition temperature of the cross-link

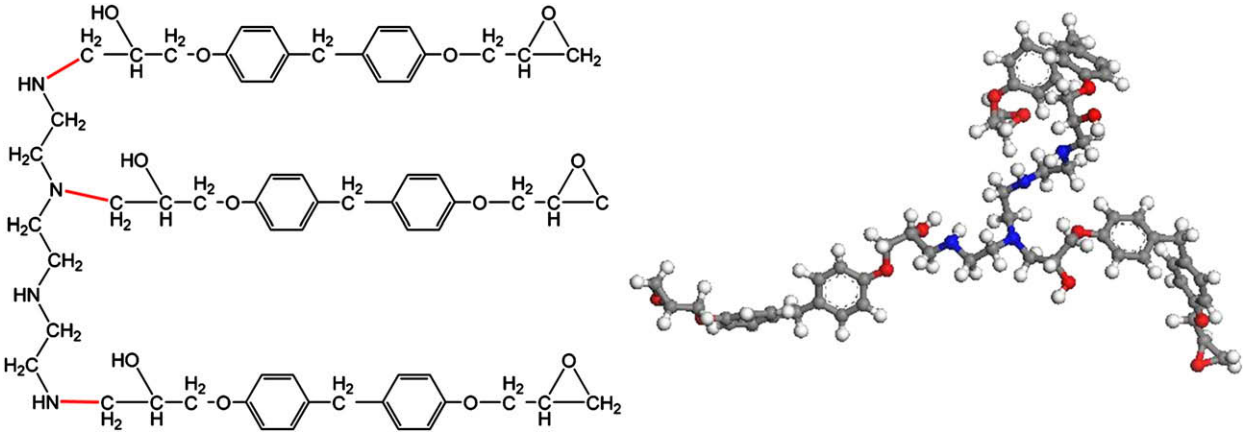

Fig. 5. Representative molecule.

Table 2
Cross-linked network effects in cross-linked epoxy simulation.

	Cross-linked epoxy	Non-cross-linked epoxy
Young's modulus [GPa]	3.362	1.823
Shear modulus [GPa]	1.222	0.657
T_g [K]	388	–

producing method and a representative molecule method are obtained and compared in Table 1. As can be seen, the values of the representative molecule method coincide with those of the cross-link producing method and are also in good agreement with the values calculated in the previous MD simulation and experimental observations. Therefore, the present representative cross-linked epoxy unit was used in all the MD simulations for this study.

In order to check the effects of the cross-linked network, an extra molecular unit cell composed of the same number of EPON 862® and TETA® molecules without any cross-linked network, was constructed. Using the Parrinello–Rahman method, the elastic modulus of the unit cell was obtained and compared. As shown in Table 2, the two unit cells show very different characteristics to each other, and the mechanical properties of the cross-linked epoxy are two times higher than those of the non-cross-linked epoxy.

In order to check the effects of the cross-linked network, the glass transition temperature, T_g, is also estimated because T_g is the one of the properties that shows the characteristics of the polymers. The glass transition temperature T_g is estimated from the relation of density–temperature and mean square displacement (MSD) during cooling-down simulation as shown in Fig. 6. The density–temperature relation is changed at near 390 K as shown in Fig. 6(a) and the gap of MSD around 390 K is larger than those at other temperatures. The density of the cell at each temperature from 500 K to 320 K is obtained in each equilibrium state. The density and MSD values should be obtained from equilibrium state. The equilibrium of the cell near the T_g is more important to get the exact values of T_g. So the equilibrium of the cells at each temperature can be confirmed from the running average of the density in Fig 7.

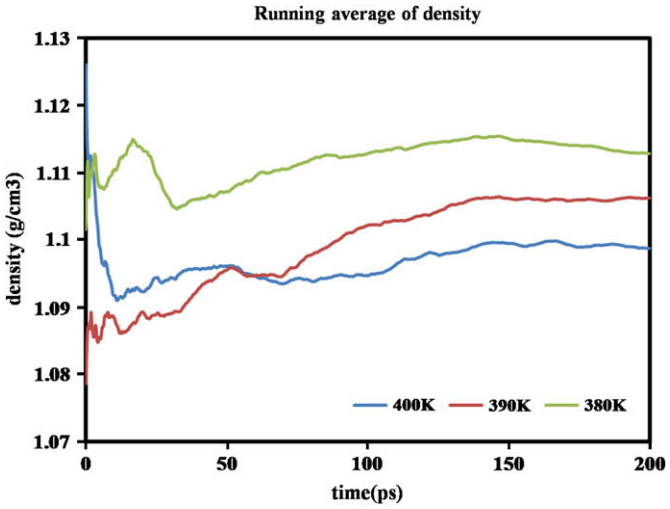

Fig. 7. The equilibrium near the T_g can be confirmed from the running average of density.

4. MD simulations for alumina/epoxy nanocomposites

4.1. Unit cell compositions

Based on the representative cross-linked molecules obtained from the previous section, the particle size effects of alumina/epoxy nanocomposites have been investigated to estimate the effects of the particles in nanocomposites, 7 unit cells, having different particle sizes. A matrix of composites is composed of a number of the representative cross-linked epoxy units constructed in the previous part, and a spherical alumina (Al_2O_3) particle was embedded at the center of the unit cell as shown in Fig. 8. No surface treatment of the alumina particle was considered and only VdW and electrostatic interactions are described between the alumina particles and the surrounding matrix.

In cell construction, the target conditions of the cells such as volume fraction and target density should be defined first. And then, lower density unit cell including the polymers and particle is constructed. After that, a repeated minimization and dynamics are applied to the cell until the density of the cell becomes the target density as the size of the cell is modified. In this study, the radius of the particles ranges from 6 to 10 Å and the number of representative cross-linked molecules included in the cells was defined considering the fixed volume fraction, 0.055. The target density of all unit cells was 1.23 g/cm^3 [21] and the details of the cell compositions are arranged in Table 3. After the cells' construction, all the unit cells were equilibrated at 300 K and 1 atm using 900 ps of NPT simulation using the Andersen–Berendsen method.

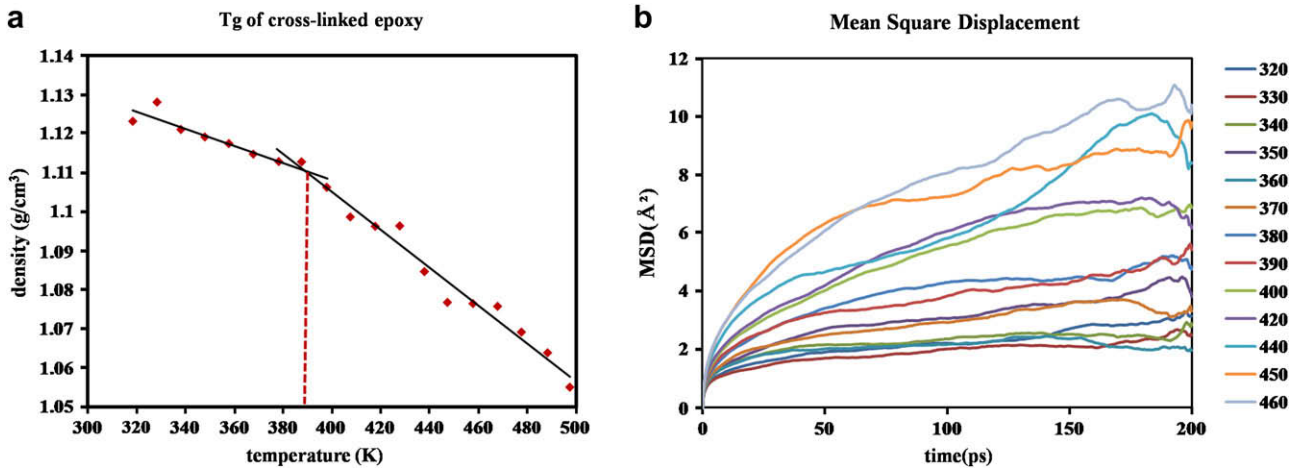

Fig. 6. T_g of cross-linked epoxy can be estimated by relation of density and temperature (a) and mean square displacement (b) during cooling-down simulation.

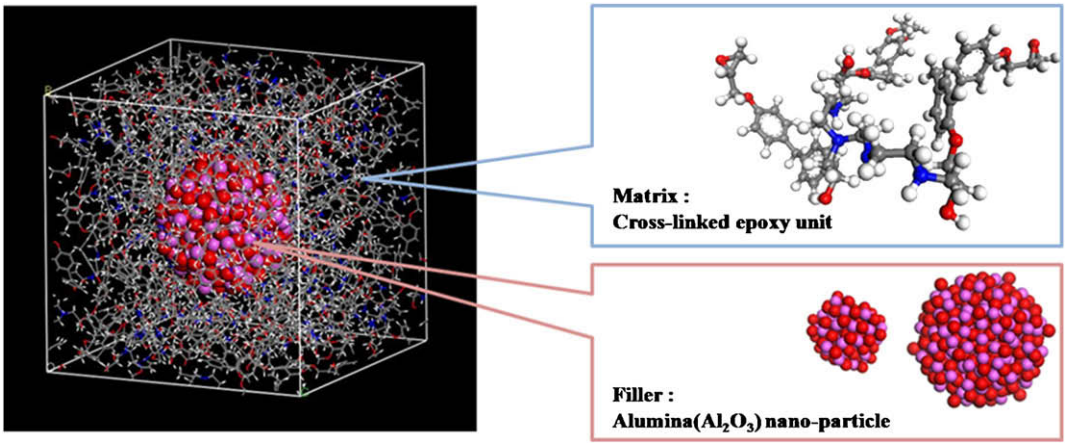

Fig. 8. The nanocomposites unit cell consists of the cross-linked epoxy unit as matrix and alumina particles as the filler.

4.2. Simulation results

The elastic modulus of each unit cell structure is obtained from the Parrinello–Rahman method, and the results of five different simulations in each case are averaged for reliable computational accuracy. The average and deviations of the elastic modulus obtained from five different simulations are shown in Table 4. As the deviations of cases 1, 3, 6 and 7 are larger than those of the other cases, five more different simulations are performed to ensure the statistically accuracy. The deviations of ten different results are smaller than that of five results and the averaged values of those are almost the same with the average of five results.

In Fig. 9, both Young's and shear moduli of nanocomposites, having different particle radii, are compared with the scattering bars. As shown in Fig. 9, both moduli show an enhanced reinforcing effect as the particle radius decreases, and this tendency coincides with the experimental observations [5]. The maximum value of the modulus of nanocomposites at the particle radius of 6.0 Å is 180% higher than those from using pure epoxy.

5. Efficient scale bridging method

5.1. Effective interface model

In order to efficiently predict the particle size effect of the present nanocomposites models, a sequential scale bridging method for dilute nanocomposites [22] was adopted. With this method, an effective interface was incorporated as a characteristic phase which describes the size-dependent elastic modulus of nanocomposites with the exponential function of particle radius.

Following the previous bridging method, nanocomposites can be modeled as a three phase heterogeneous structures (particle, matrix and interface) and an effective stiffness matrix of the nanocomposites can be obtained as shown below.

Table 3
Compositions of epoxy/alumina nanocomposites unit cells.

	Particle radius [Å]	No. of EPON862®	No. of TETA®	Cell length [Å]	Volume fraction
CASE 1	6.0	27	9	25.34	0.055
CASE 2	7.0	45	15	29.64	0.055
CASE 3	7.9	63	21	33.47	0.055
CASE 4	8.2	72	24	34.80	0.055
CASE 5	8.6	81	27	36.38	0.055
CASE 6	8.9	90	30	37.70	0.055
CASE 7	10.0	126	42	42.30	0.055

$$\boldsymbol{C} = \boldsymbol{C}_m + \left[\left(f_p + f_i\right)(\boldsymbol{C}_i - \boldsymbol{C}_m)\boldsymbol{A}_{pi}^{di} + f_p(\boldsymbol{C}_p - \boldsymbol{C}_i)\boldsymbol{A}_p^{di}\right] \left[f_m\boldsymbol{I} + (f_p + f_i)\boldsymbol{A}_{pi}^{di}\right]^{-1} \quad (4)$$

where the capital letter $\boldsymbol{C}$ is the fourth order stiffness tensor and f is the volume fraction of each phase subscribed as p, m, i corresponding to the particles, matrix and interface respectively and $\boldsymbol{I}$ is the identity tensor. $\boldsymbol{A}_p^{di}$ and $\boldsymbol{A}_{pi}^{di}$ are the fourth order dielectric strain concentration tensors of particles and effective particles (particles including their interfaces) given by

$$\boldsymbol{A}_p^{di} = \boldsymbol{I} - \boldsymbol{S}\left[\boldsymbol{S} + (\boldsymbol{C}_p - \boldsymbol{C}_m)^{-1}\boldsymbol{C}_m\right]^{-1}$$

$$\boldsymbol{A}_{pi}^{di} = \boldsymbol{I} - \boldsymbol{S}\left\{\frac{f_p}{f_i + f_p}\left[\boldsymbol{S} + (\boldsymbol{C}_p - \boldsymbol{C}_m)^{-1}\boldsymbol{C}_m\right]^{-1} + \frac{f_i}{f_i + f_p}\left[\boldsymbol{S} + (\boldsymbol{C}_i - \boldsymbol{C}_m)^{-1}\boldsymbol{C}_m\right]^{-1}\right\} \quad (5)$$

where $\boldsymbol{S}$ is the Eshelby's tensor [23] for isotropic spherical inclusion given by

$$\boldsymbol{S}_{1111} = \boldsymbol{S}_{2222} = \boldsymbol{S}_{3333} = \frac{7 - 5\nu}{15(1 - \nu)}$$

$$\boldsymbol{S}_{1112} = \boldsymbol{S}_{2233} = \boldsymbol{S}_{1133} = \frac{5\nu - 1}{15(1 - \nu)}$$

$$\boldsymbol{S}_{1212} = \boldsymbol{S}_{2323} = \boldsymbol{S}_{3131} = \frac{4 - 5\nu}{15(1 - \nu)} \quad (6)$$

where ν is Poisson's ratio of the matrix.

Table 4
The deviations become smaller as the simulation times increase.

	E (5 results)		E (10 results)		G (5 results)		G (10 results)	
	AVG	STDEV	AVG	STDEV	AVG	STDEV	AVG	STDEV
CASE 1	5.87	0.812	6.22	0.715	2.18	0.335	2.32	0.304
CASE 2	5.68	0.227	–	–	2.1	0.099	–	–
CASE 3	5.61	0.857	5.14	0.834	2.11	0.359	1.91	0.347
CASE 4	4.77	0.365	–	–	1.76	0.147	–	–
CASE 5	4.50	0.373	–	–	1.66	0.172	–	–
CASE 6	4.51	0.582	4.42	0.459	1.66	0.235	1.64	0.186
CASE 7	4.14	0.648	4.00	0.527	1.52	0.250	1.47	0.207

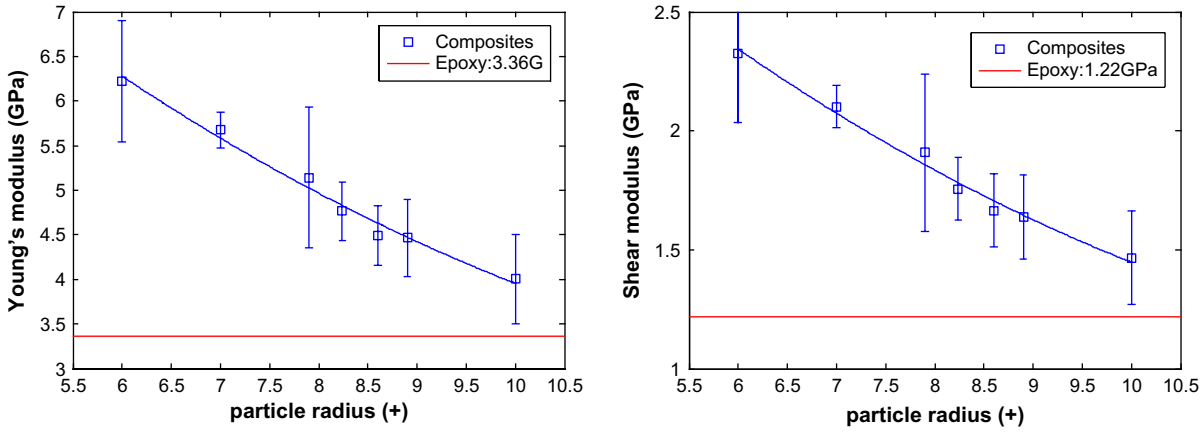

Fig. 9. Young's modulus and shear modulus of composites increase up to 180% as the size of the particles decreases. The red lines are the modulus of pure epoxy. (For interpretation of the references to colour in this figure legend, the reader is referred to the web version of this article.)

In order to utilize Eqs. (4) and (5) to obtain the elastic modulus of nanocomposites with size effects, the volume fraction and stiffness matrix have to be defined. As was demonstrated in the former bridging process [22], the volume fraction of the effective interface was decided from the radial density distribution of the matrix polymer, and the stiffness matrix of the interface was obtained using an inversion method. Other variables in Eqs. (4) and (5) can be obtained from MD simulations, cell compositions and shapes of the particles and interfaces (both the shape of the particles and the effective particles are concentric and spherical).

Radial density distributions of EPON862®/TETA® cross-linked epoxy and alumina particle are shown in Fig. 10. There exists a distinguishably high peak of matrix near the surface of the particle. This highly concentrated region (adsorption layer) can be regarded as a different phase from the pure matrix phase and this makes the definition of the effective interface reasonable. Defining the outer diameter of the adsorption layer as 4 Å, the thickness of the interface was calculated from the radial distance of the matrix and the particle as shown below.

$$r_{\text{matrix}} = r_{\text{peak}} + t_{\text{absorption}} \tag{7}$$

$$t_{\text{interface}} = r_{\text{matrix}} - r_{\text{particle}} \tag{8}$$

The thickness of the interface in each composite unit cells is listed in Table 5 and found to be almost 6.8 Å.

After defining the volume fraction of the interface, the stiffness matrix of the interface was then calculated from the inversion form, defined as

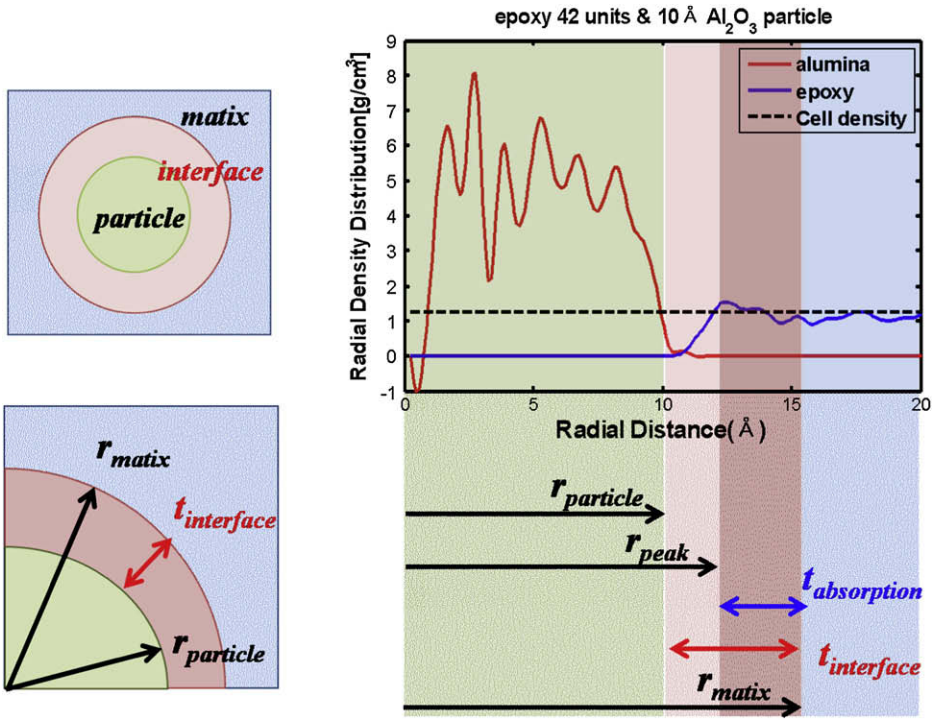

Fig. 10. Effective continuum model of nanocomposites can be divided into three parts, matrix, interface and particle. The thickness of the effective interface and radius of matrix can be determined from the radial density distribution of the composites.

Table 5
Thickness of the interface and radius of particles and the matrix.

	r_{peak} [Å]	$t_{absorption}$ [Å]	r_{matrix} [Å]	$r_{particle}$ [Å]	$t_{interface}$ [Å]	$E_{interface}$ [GPa]	$G_{interface}$ [GPa]
CASE 1	8.65	4.0	12.65	6.0	6.68	9.46	3.61
CASE 2	9.85	4.0	13.85	7.0	6.85	10.4	3.94
CASE 3	10.25	4.0	14.25	7.9	6.35	9.45	3.70
CASE 4	11.05	4.0	15.05	8.2	6.85	7.70	2.92
CASE 5	11.35	4.0	15.35	8.6	6.75	6.48	2.47
CASE 6	11.75	4.0	15.75	8.9	6.85	6.60	2.45
CASE 7	12.45	4.0	16.45	10.0	6.45	4.42	1.67
Matrix	–	–	–	–	–	3.36	1.22

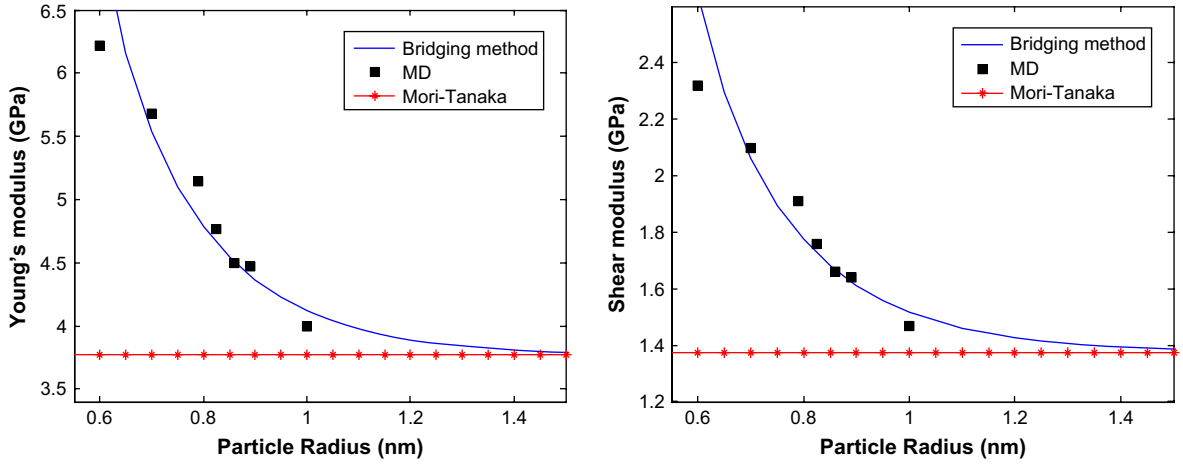

Fig. 11. Elastic modulus obtained from the effective interface model agrees well with MD simulation results, and the model can describe the particle's size effects quite efficiently.

$$\left\{\left[c_p\boldsymbol{C}_p\boldsymbol{A}_p^{di}-c_m(\boldsymbol{C}-\boldsymbol{C}_m)-c_p\boldsymbol{C}\boldsymbol{A}_p^{di}\right]\boldsymbol{S}(\boldsymbol{C}_m)^{-1}+c_i\boldsymbol{I}\right\}\boldsymbol{C}_i = c_i\boldsymbol{C}+\left[c_p\boldsymbol{C}_p\boldsymbol{A}_p^{di}-c_m(\boldsymbol{C}-\boldsymbol{C}_m)-c_p\boldsymbol{C}\boldsymbol{A}_p^{di}\right](\boldsymbol{S}-\boldsymbol{I}) \quad (9)$$

In Eq. (9), only average values of the elastic modulus of the nanocomposites in the five times MD run are used to obtain the elastic modulus of the effective interface. Under the assumption that the effective interface is isotropic, both Young's modulus and the shear modulus of the interface were fitted into the exponential function of the particle radius, and the stiffness matrix of the interface was reconstructed as a function of the particle radius. Then, the elastic modulus of the nanocomposites at various particle radii and volume fractions can be efficiently obtained from Eqs. (4) and (5).

5.2. Results and discussions

The elastic moduli obtained from the bridging methods are compared with the MD simulation results, and can be seen in Fig. 11. Both Young's modulus and shear modulus of the nanocomposites accurately follow the MD simulation results and gradually converge to the results of Mori–Tanaka method's [15] estimates. Based on the interface modulus obtained from the

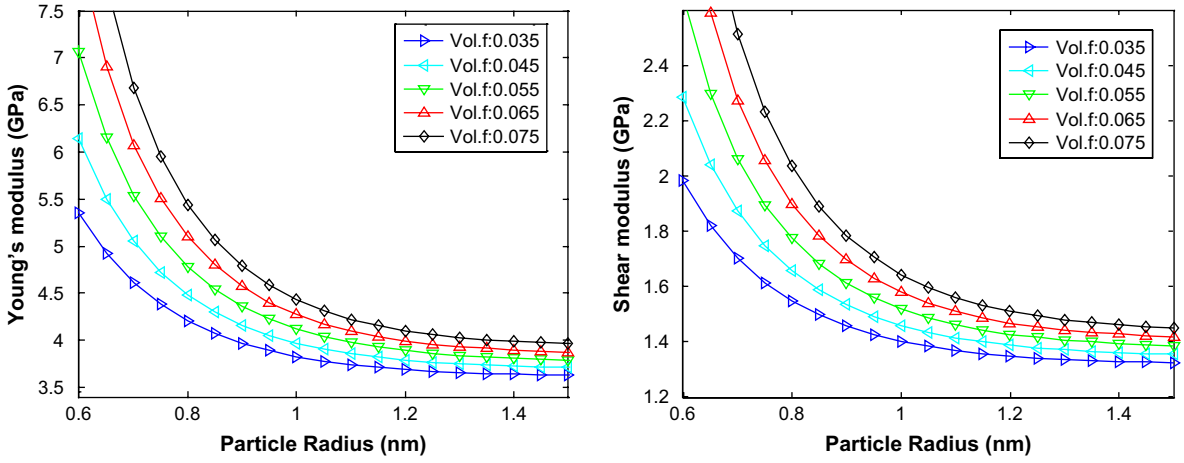

Fig. 12. The modulus of composites having various volume fractions is shown. The modulus increases as the volume fraction becomes higher.

bridging process, the elastic modulus at various volume fractions and radii were efficiently obtained, as shown in Fig. 12. In the case of thermoset polymer-based nanocomposites, the difference from the thermoplastic matrix, not only in particle composition, size and surface treatment, but also in the degree of cross-linked network can be an important design variable. Therefore, the application of the efficient bridging method combined with rigorous consideration of the cross-linked network of matrix polymer in atomistic scale can be a useful analytical approach for the design of real epoxy-based nanocomposites materials.

6. Conclusions

In this study, the size effect of nanoparticles on the mechanical properties of thermoset polymer matrix-based nanocomposites has been demonstrated by MD simulations and a sequential scale bridging method. In order to closely consider the cross-linked network effects of epoxy, an intra-atomic potential based cross-linking simulation based approach was adopted, and a representative cross-linked molecule unit method was proposed for an efficient cross-linking simulation. The suggested method was validated by comparing the experimental and analytical results. Using the representative cross-linked unit, Al_2O_3/Epoxy nanocomposites were constructed, and the size effects of Al_2O_3 particles on the mechanical properties were investigated. As a result, an enhanced reinforcing effect was observed in the smaller particle reinforced nanocomposites. Using the MD simulation results, a multi-scale bridging method was applied to efficiently estimate the elastic modulus of nanocomposites at various particle radii and volume fractions. By using the method proposed in this study, the design and analysis of the nanocomposites considering the microstructures and change of microscopic material properties can be performed efficiently.

Acknowledgments

This work was supported by the Korea Science and Engineering Foundation (KOSEF) grant funded by the Korea government (MOST) (No. R0A-2008-000-20109-0).

References

[1] Odegard GM, Clancy TC, Gates TS. Polymer 2005;46:553–62.
[2] Li GZ, Wang L, Toghiani H, Daulton TL, Pittman Jr CU. Polymer 2002;43:4167–76.
[3] Mark JE, Abou-Hussein R, Sen TZ, Kloczkowski A. Polymer 2005;46:8894–904.
[4] Allegra G, Raos G, Vacatello M. Progress in Polymer Science 2008;33:683–731.
[5] Cho J, Joshi MS, Sun CT. Composites Science and Technology 2006;66:1941–52.
[6] Wu C, Xu W. Polymer 2006;47:6004–9.
[7] Wu C, Xu W. Polymer 2007;48:5802–12.
[8] Hamerton I, Howlin BJ, Klewpatinond P, Shortley HJ, Takeda S. Polymer 2006;47:690–8.
[9] Yarovsky I, Evans E. Polymer 2002;43:963–9.
[10] Komarov PV, Chiu YT, Chen SM, Khalatur PG, Reineker P. Macromolecules 2007;40:8104–13.
[11] Liang Z, Gou J, Zhang C, Wang B, Kramer L. Materials Science and Engineering A 2004;365:228–34.
[12] Zhu R, Pan E, Roy AK. Materials Science and Engineering A 2007;447:51–7.
[13] Alperstein D, Dodiuk H, Kenig S. Acta Polymerica 1998;49:594–9.
[14] Zeng QH, Yu AB, Lu GQ. Progress in Polymer Science 2008;33:191–269.
[15] Mori T, Tanaka K. Acta Metallurgica 1973;21(5):571–4.
[16] Accelrys Inc., San Diego, www.Accelrys.com.
[17] Bharadwaj RK, Berry RJ, Farmer BL. Polymer 2000;41:7209–21.
[18] Parrinello M, Rahman A. Journal of Chemical Physics 1982;76(5):2662–6.
[19] Parrinello M, Rahman A. Physical Review Letters 1980;45:1196–9.
[20] Fan HB, Yeun MMF. Polymer 2007;48:2174–8.
[21] Literature from resolution performance products; 2005. Available from: www.resins.com/resins/am/pdf/SC0772.pdf.
[22] Yang S, Cho M. Appled Physics Letters 2008;93(4):043111.
[23] Eshelby JD. Proceedings of the Royal Society A 1957;241:379–98.